Title: Aboveground and belowground contributions to ecosystem respiration in a temperate deciduous forest

Authors: Xiuping Liu[1], Wenxu Dong[1], Jeffrey D. Wood[2], Yuying Wang[1], Xiaoxin Li[1], Yuming Zhang[1], Chunsheng Hu[1], Lianhong Gu[3]

Affiliations:

[1] Key Laboratory of Agricultural Water Resources, Hebei Key Laboratory of Soil Ecology, Center for Agricultural Resources Research, Institute of Genetics and Developmental Biology, Chinese Academy of Sciences, Shijiazhuang, 050021, China

[2] School of Natural Resources, University of Missouri, Columbia, MO, 65211, USA

[3] Environmental Sciences Division and Climate Change Science Institute, Oak Ridge National Laboratory, Oak Ridge, TN, 37831, USA

Author for correspondence: Chunsheng Hu, Lianhong Gu

Email: cshu@sjziam.ac.cn, lianhong-gu@ornl.gov

Word counts： 4733 (Introduction: 724, Materials and Methods: 1456, Results: 661, Discussion: 1755, Conclusion:131, and Acknowledgements: 46)

Number of tables: 3

Number of figures: 10

Abstract

In this study, we developed a three-way carbon dioxide (CO_2) flux-partitioning algorithm that separates net ecosystem exchange (NEE) into aboveground plant respiration (R_{above}), belowground root and soil respiration (R_{below}), and gross primary production (GPP). We applied this algorithm to a coupled dataset of continuous chamber-measured soil respiration and eddy covariance (EC)-measured NEE of CO_2 in an oak-hickory (*Quercus-Carya*) deciduous broadleaf forest from 2006 to 2015. We found that on annual time scale, R_{below} dominated over R_{above} with the former accounting for 66.9-86.4% and the latter 13.6-33.1%, of the total ecosystem respiration (R_{eco}). The ratio of R_{below} to R_{above} varied seasonally, ranging from 1.77 to 7.25 in growing season, and 1.02 to 4.57 in non-growing season. The temperature sensitivity (E_0) of R_{below} was significantly higher than that of R_{above}, and E_0 of R_{eco} responded differently to air and soil temperature. Over the whole study period, annual mean R_{above}, R_{below}, and GPP were 243, 806, and 1170 g C m^{-2}, respectively, with annual R_{eco} accounting for 89.6% of GPP, of which 68.8% was lost as R_{below} and 20.8% lost as R_{above}, and leaving only 10% of the carbon fixation in ecosystems. These estimates, however, did not consider potential light inhibition of leaf respiration. If we accept the presence of light inhibition, then the daytime three-way partitioning method would underestimate annual R_{above} by 20.4% whereas the nighttime method would overestimate R_{above} by 23.9% and GPP by 4.7%, compared with estimates accounting for light inhibition in leaves.

Key words: net ecosystem exchange; soil respiration; flux partitioning; temperature sensitivity; MOFLUX

1. Introduction

Forests contain large stocks of carbon which represent the long-term, accumulated difference between two massive fluxes—photosynthesis and respiration. As a result, forests exert significant leverage on the global carbon cycle and greenhouse gas balance (Hutyra et al., 2008; Raj et al., 2016). Determination of photosynthesis (gross primary production, GPP) and respiration (ecosystem respiration, R_{eco}) in forest ecosystems will help elucidate the key elements modulating the carbon-climate connection (Moore et al., 2018). A major challenge in understanding and predicting terrestrial carbon balance is that the commonly-used variable ecosystem respiration (R_{eco}) integrates several different soil and plant processes, each of which is mediated by different ecophysiological mechanisms with different sensitivity to environmental drivers (Hutyra et al., 2008; Ogee et al., 2004). A necessary step towards overcoming this challenge is to partition R_{eco} into its aboveground plant respiration (R_{above}) and belowground root and soil respiration (R_{below}), which will lead to better interpreting the seasonal and interannual variations in R_{eco} and their environmental controls (Wang et al., 2017; Xu and Baldocchi, 2004).

Chamber-based methods have been widely used to measure foliar, trunk, and soil plus root respiratory fluxes in R_{eco} (Gaumont-Guay et al., 2006; Wang et al., 2010). However, modifications of the soil/plant environment (e.g., temperature and humidity) in chambers may cause errors (Ohkubo et al., 2007; Wohlfahrt et al., 2005a), and uncertainties in upscaling from chamber to ecosystem level may also introduce biases (Bolstad et al., 2004; Miyama et al., 2006). Partitioning flux tower measurements of net CO_2 exchange is another commonly used method for estimating GPP and R_{eco} (Lasslop et al., 2010; Reichstein et al., 2005), which is usually based on temperature response functions (Lasslop et al., 2012). However, R_{eco} is the sum of R_{above} and R_{below} which respond differently to local environmental conditions such as temperature and moisture (Brito et al., 2013). For example, R_{below} is mainly controlled by soil temperature and moisture (Gilmanov et al., 2013), whereas air temperature controls R_{above} (Jassal et al., 2007). Additionally, the Kok effect (Kok, 1948; Kok, 1949), which hypothesizes existence of photoinhibition on leaf respiration, should only affect R_{above}, but not R_{below} (Buckley et al., 2017; Heskel et al., 2013). Therefore, common CO_2 flux partitioning algorithms (Lasslop et al., 2010; Reichstein et al., 2005) using a single-source respiration model is thus an oversimplification which may result in biased R_{eco}

estimates (Wohlfahrt and Galvagno, 2017). Moreover, eddy-covariance (EC) systems measure the CO_2 fluxes above the canopy, and the transport of CO_2 molecules from soil surface to the sensor declines the coupling of observed fluxes with temperature (Lasslop et al., 2012; Paul-Limoges et al., 2017). Therefore, separating R_{eco} components and using proper driving temperatures are necessary to better understanding the role of R_{eco}, and can reduce uncertainties in the inferred GPP (Oikawa et al., 2017; Wohlfahrt and Galvagno, 2017).

Continuous automated chamber measurements of R_{below}, in conjunction with EC-measured R_{eco}, have been used to distinguish the responses of belowground and aboveground components of R_{eco} to seasonal variations in their environmental controls (Jassal et al., 2007; Rana et al., 2018). When root exclusion methods are combined with soil chamber measurements, R_{below} can be further separated into heterotrophic and autotrophic respiration (Dyukarev, 2017; Järveoja et al., 2018). However, these studies did not jointly partition the net ecosystem exchange (NEE) of CO_2 into photosynthesis and different components of R_{eco} (Oikawa et al., 2017). Since R_{eco} is composed of multiple respiration sources with differing driving temperatures, estimates of GPP and R_{eco} may be biased with a paritioning approach conceptualizing R_{eco} to originate from a single source. It is therefore necessary to partition R_{eco} based on environmental factors at the respiratory sources to better understand forest ecosystem carbon dynamics.

The present study intends to address the issues identified above. Our specific objectives are to: (1) develop a three-way flux-partitioning algorithm that partitions NEE into R_{above}, R_{below}, and GPP with explicit representation of temperature sensitivities of different respiratory sources; (2) quantify the temporal dynamics in R_{above}, R_{below}, and GPP, and compare R_{above}, R_{below}, and GPP derived from daytime NEE and soil respiration to those obtained with nighttime data; and (3) calculate the potential Kok effect on the estimates of R_{above} and GPP. We used decade-long (2006-2015) dataset of hourly continuous chamber measurements of soil respiration in conjunction with EC observations of net ecosystem carbon exchange at the Missouri Ozark AmeriFlux (MOFLUX) site, USA.

2. Materials and methods

2.1. Site description

The measurements were made in oak-hickory (*Quercus-Carya*) forest at MOFLUX site

(38°44′N, 92°12′W). The soils are Weller silt loam and Clinkenbeard very flaggy clay loam (Young et al., 2001), and white oak (*Quercus alba*), black oak (*Q. velutina*), shagbark hickory (*Carya ovata*), and sugar maple (*Acer saccharum*) are the dominant tree species. The stand density is about 583 trees ha^{-1}, canopy height ranges from 18 to 20 m, and the seasonal peak leaf area index is about 3.2 to 3.7 m^2 m^{-2}. For further details about the site, see Gu et al. (2006), Yang et al. (2010), and Liu et al. (2020).

2.2. NEE and soil respiration measurements

NEE was measured by EC technique while soil respiration (including root and soil respiration) was measured by automated chambers (Liu et al., 2020). The data presented here were collected between 2006 and 2015.

Half-hourly NEE values were calculated using fundamental equation of EC (Gu et al., 2012) and the quality checked with criteria defined by Mauder and Foken (2011). The data was partitioned into daytime and nighttime sets using an incoming solar radiation threshold of 20 W m^{-2}. For daytime periods, data gaps due to instrument malfunction, power failure, and calibration schedule were filled using the mean diurnal variation (MDV) approach (Gu et al., 2016). And for the nighttime, the objective friction velocity filtering approach of Gu et al. (2005) was used to screen for data affected by low-turbulence conditions. In general, nighttime NEE (NEE_{night}) represents soil and plant respiration (nighttime R_{eco}, $R_{eco,night}$) because plants do not photosynthesize at night. However, our data measured by EC was not consistently higher than chamber-measured nighttime R_{below} ($R_{below,night}$). NEE_{night} could be underestimated during atmospherically stable nights (Miao et al., 2017). To evaluate this, we created graphs to describe the changes in the difference between NEE_{night} and $R_{below,night}$ at low windspeed (Fig. 1). In summer, NEE_{night} was about 29.9% lower than $R_{below,night}$ when windspeed below 2.66 m s^{-1}, while in winter, 13.9% of NEE_{night} was lower than $R_{below,night}$ when windspeed below 1.77 m s^{-1} (Fig. 1). Our data showed that NEE_{night} was possibly underestimated due to inadequate turbulent mixing at low windspeed. Thus, the Lloyd and Taylor (1994) model was made using data at high windspeed, replacing data at low windspeed, that is, we discarded sporadic records of NEE_{night} that were less than $R_{below,night}$ when summer and winter windspeed exceeded 2.66 and 1.77 m s^{-1}, and developed model for NEE_{night} to predict data when windspeed below 2.66 and 1.77 m s^{-1}, respectively. Meanwhile, R_{below} was gap-filled using the Lloyd and Taylor (1994) model, and gaps in air temperature, atmospheric vapor

pressure deficit (VPD), and global radiation were filled by the marginal distribution sampling (MDS) method.

2.3. R_{above}, R_{below}, and GPP estimation

The net flux of carbon from aboveground ecosystem compoents is defined as the net aboveground exchange (NAE), the difference between the CO_2 assimilation by photosynthesis (i.e., gross primary productivity, GPP) and foliar and trunk respiration (aboveground plant respiration, R_{above}). Following the micrometeorological convention, we define R_{above} and R_{below} as positive and GPP as negative, and a net flux of CO_2 to the atmosphere represents a positive NAE or NEE.

$$NAE = NEE - R_{below} = -\frac{\alpha\beta R_g}{\alpha R_g + \beta} + R_{above} \quad (1)$$

$$R_{above} = R_{ref} exp\left(E_0\left(\frac{1}{T_{ref} - T_0} - \frac{1}{T_{air} - T_0}\right)\right) \quad (2)$$

where NAE (μmol m^{-2} s^{-1}) is net aboveground exchange; NEE (μmol m^{-2} s^{-1}) is net ecosystem exchange, measured with EC flux tower; R_{below} (μmol m^{-2} s^{-1}) is belowground soil respiration (including litter, soil, and root respiration), measured with automated chambers; R_{above} (μmol m^{-2} s^{-1}) is aboveground plant respiration (the sum of foliar and trunk respiration), modelled with exponential regression equation (Lloyd and Taylor, 1994); $\frac{\alpha\beta R_g}{\alpha R_g + \beta}$ is a rectangular hyperbolic light-response curve, used to estimate GPP; α (μmol J^{-1}) is the canopy-scale quantum yield; β (μmol m^{-2} s^{-1}) is the maximum rate of CO_2 uptake of the canopy at light saturation (for details, see Lasslop et al. (2010)); R_g (W m^{-2}) is global radiation; R_{ref} (μmol m^{-2} s^{-1}) is the basal respiration at reference temperature (T_{ref}) of 15°C; E_0 (K) is temperature sensitivity; T_{air} (°C) is air temperature; and T_0 (°C) is constant (−46.02°C).

Using the half-hourly chamber-measured soil respiration and EC-measured NEE of CO_2, the flux partitioning algorithms of Lasslop et al. (2010) were applied to separate NAE (the difference between NEE and R_{below}) into R_{above} and GPP. This apporach is hereafter referred to as the daytime NEE and soil respiration (DNS) method. It is reasonable to assume that R_{above} responds to air temperature measured above canopy while R_{below} responds to soil temperature and moisture. The air temperature-sensitive portion of NEE was assigned to R_{above}, the soil temperature and moisture- sensitive portion of NEE was assigned to R_{below}, and the R_g-sensitive portion of NEE was assigned to GPP. At first, NAE was derived from NEE by subtracting R_{below}, which was measured with automated chambers. The GPP and R_{above} portions were then modeled

as a function of NAE, R_g, and T_{air}, using the rectangular hyperbola and exponential function, respectively. E_0 was estimated every 7 days with a 15-day moving window using nighttime NAE and T_{air}. With the fixed E_0, the remaining parameters (α, β, and R_{ref}) were estimated by fitting the entire model (Eq. 1) to the daytime data (daytime NAE, T_{air}, T_{ref}, VPD, and R_g). Based on the intercept of a light-response curve fit to daytime observations, GPP and daytime R_{above} ($R_{above,day}$) were estimated from the regression of daytime NAE against R_g (Eq. 1). The parameters E_0 and R_{ref} were then used to extrapolate nighttime R_{above} ($R_{above,night}$) with T_{air} (Eq. 2), and total R_{above} was the sum of $R_{above,day}$ and $R_{above,night}$. Daily and annual total R_{above}, R_{below}, and GPP calculated from summing half-hourly R_{above}, R_{below}, and GPP, respectively.

To evaluate and compare the performance and accuracy of the partitioning methods, the flux partitioning algorithms for estimating daytime respiration from nighttime measurements were also applied to separate NEE into R_{above}, R_{below}, and GPP, hereafter referred to as the nighttime NEE and soil respiration (NNS) method. Based on the assumption that $R_{above,day}$ was of similar magnitude and responsiveness as $R_{above,night}$, $R_{above,night}$ was first calculated as the difference between NEE_{night} and $R_{below,night}$, the parameters E_0 and R_{ref} were estimated using the exponential regression of $R_{above,night}$ with nighttime T_{air} and then were used to extrapolate $R_{above,day}$ with daytime T_{air} (Eq. 2), and total R_{above} was the sum of $R_{above,day}$ and $R_{above,night}$. GPP was estimated by subtracting $R_{above,day}$ and daytime R_{below} ($R_{below,day}$) from daytime values of NEE.

The Lloyd-Taylor model (Eq. 2) was used to describe the response of half-hourly R_{above} and R_{below} to air and soil temperature, respectively. In addition, we also simulated the relationship of R_{eco} with air and soil temperature to compare the difference between air and soil temperature sensitivity. The parameter E_0 characterizes the temperature sensitivity of respiration processes (Kruse et al., 2011). T_{ref} and T_0 are the same as that in Eq. 2. One-way ANOVA was performed to examine the difference in temperature sensitivity of R_{above}, R_{below}, and R_{eco} (at $p<0.05$).

It is known that leaf respiration is often inhibited by light, that is, leaf respiration is lower during the day than at night for the same temperature (Tcherkez et al., 2009), so daytime R_{eco} ($R_{eco,day}$) is likely to differ from that at night (Janssens et al., 2001). The extrapolation of R_{eco} would underestimate $R_{eco,night}$ by DNS method (Keenan et al., 2019) and overestimate $R_{eco,day}$ and GPP by NNS method (Wohlfahrt et al., 2005b). Keenan et al. (2019) calculated reference respiration (R_{ref}) separately from daytime and

nighttime observations, and used the difference between them as an estimate of the apparent inhibition of daytime ecosystem respiration. Available evidence, however, indicates that the Kok effect could only inhibit R_{above} but not R_{below} (Tcherkez et al., 2017; Wohlfahrt et al., 2005b), the flux partitioning algorithm (Keenan et al., 2019) incorporating R_{below} into the light inhibition of foliar respiration would aggravate photoinhibition effect and thus under- or overestimate inhibition biases in both R_{above} and GPP. Herein, using the flux partitioning algorithms of Keenan et al. (2019), we calculated the estimation bias in R_{above} and GPP resulted from neglecting the light inhibition of leaf respiration in the DNS and NNS method. At first, we estimated nighttime R_{ref} from nighttime data as in the NNS method, and estimated daytime R_{ref} from daytime data as in the DNS method, and then applied daytime R_{ref} to estimate daytime R_{above} only and applied nighttime R_{ref} to estimate nighttime R_{above}. The GPP in the daytime method was estimated from the light–response curve, and GPP in the nighttime method was estimated by subtracting $R_{above,day}$ and $R_{below,day}$ from daytime values of NEE. That is, the parameters E_0 and nighttime R_{ref} were estimated from nighttime data ($R_{above,night}$ and T_{air}) and parameters α, β, and daytime R_{ref} were estimated from dayttime data ($R_{above,day}$, T_{air}, T_{ref}, VPD, and R_g). The estimates of R_{above} and GPP were compared with those estimated from DNS and NNS method to obtain the estimation bias.

3. Results

3.1. Measured NEE

Daily mean NEE averaged -0.92±0.14 g C m^{-2} d^{-1} (mean±S.E.) from 2006 to 2015 (Fig. 2). Daily NEE was positive during the non-growing season, but declined rapidly and became negative at the start of growing season, and then rise to positive as the growing season progressed (Fig. 2). Annual mean net CO_2 uptake (i.e. NEE) was 618 g C m^{-2} $year^{-1}$ with the maximum in 2013 (807 g C m^{-2} $year^{-1}$) and minimum in 2012 (354 g C m^{-2} $year^{-1}$) (Fig. 2).

3.2. Estimated R_{above} and measured R_{below}

Daily mean R_{above} (2006–2015) estimated by DNS ($R_{above\text{-}DNS}$) and NNS ($R_{above\text{-}NNS}$) method averaged 0.67±0.04 and 1.04±0.05 g C m^{-2} d^{-1}, respectively (Fig. 3, Table 1). Daily mean $R_{above\text{-}DNS}$ and $R_{above\text{-}NNS}$ during the non-growing season were 0.34±0.03 and 0.54±0.04 g C m^{-2} d^{-1}, and corresponding growing season R_{above} were 0.99±0.06

and 1.53±0.07 g C m^{-2} d^{-1}, respectively (Fig. 3, Table 1). Annual mean $R_{above\text{-}DNS}$ at 243±17.2 g C m^{-2} $year^{-1}$ was lower than $R_{above\text{-}NNS}$ at 378±25.3 g C g m^{-2} $year^{-1}$ with $R_{above\text{-}DNS}$ exceeding $R_{above\text{-}NNS}$ during 2006 (Fig. 4).

Daily mean R_{below} (i.e. soil respiration) measured with automated chambers averaged 2.21±0.09 g C m^{-2} d^{-1} (Fig. 3, Table 1). Seasonal changes in R_{below} followed a pattern similar to that of R_{above}. It was moderate in late spring (mean 3.31±0.06 g C m^{-2} d^{-1} in May), increased sharply to a peak in summer (mean 4.95±0.08 g C m^{-2} d^{-1} in July), and then decreased in autumn (mean 1.62±0.03 g C m^{-2} d^{-1} in October) (Fig. 3). Annual mean R_{below} was 806±38.9 g C m^{-2} $year^{-1}$ with the minimum in 2012 (540 g C m^{-2} $year^{-1}$) and maximum in 2010 (931 g C m^{-2} $year^{-1}$) (Fig. 4).

Annual mean R_{eco} estimated by DNS ($R_{eco\text{-}DNS}$) and NNS ($R_{eco\text{-}NNS}$) method averaged 1049±38.4 and 1184±29.8 g C m^{-2} $year^{-1}$, respectively (Fig. 4). The contribution of $R_{above\text{-}DNS}$ and $R_{above\text{-}NNS}$ to R_{eco} averaged 23.4% and 32.1%, while the contribution of corresponding R_{below} to R_{eco} averaged 76.6% and 67.9%, respectively (Fig. 3-4, Table1). R_{below} contributed more than R_{above} to R_{eco} at the MOFLUX site.

3.3. Estimated GPP

GPP also followed a strong seasonal pattern, monthly mean daytime GPP by DNS (GPP_{DNS}) and NNS (GPP_{NNS}) method increased from 7.07±0.51 and 7.65±0.68 g C m^{-2} d^{-1} in May up to 9.50±0.64 and 10.2±0.81 g C m^{-2} d^{-1} in June, and then decreased gradually to 2.09±0.20 and 2.24±0.34 g C m^{-2} d^{-1} in October, respectively (Fig. 5). Annual mean GPP_{DNS} and GPP_{NNS} were 1170±54.0 and 1266±57.9 g C m^{-2} $year^{-1}$, and annual GPP varied from a minimum of 781 and 860 g C m^{-2} $year^{-1}$ in 2012 to a maximum of 1368 and 1491 g C m^{-2} $year^{-1}$ in 2009, respectively (Fig. 6). At annual time scale, NNS method estimates had GPP values higher than estimates obtained from DNS method (Fig. 6).

3.4. Temperature sensitivity

The temperature sensitivities (i.e., the E_0 value) of R_{above}, R_{below}, and R_{eco} varied greatly from year to year (Table 2-3). Overall, annual mean E_0 of $R_{above\text{-}DNS}$ and $R_{above\text{-}NNS}$ averaged 197±14.8 and 186±9.95K, respectively, and annual mean E_0 of R_{below} was on average 388±32.0K (Table 2). Meanwhile, annual mean E_0 of $R_{eco\text{-}DNS}$ calculated by air and soil temperature were 234±13.8 and 346±24.1K, and corresponding E_0 of $R_{eco\text{-}NNS}$ were 225±11.3 and 334±22.2K, respectively (Table 3). Throughout the study period,

the E_0 of R_{below} greatly exceeded that of R_{above} (Fig. 7) and was thus driving the apparent temperature sensitivity of R_{eco} (Fig. 8).

3.5. Estimation bias

The R_{ref} estimated by daytime and nighttime data averaged 0.65±0.18 and 0.95±0.09 μmol m^{-2} s^{-1}, respectively (Fig. 9). When leaf respiration reduction in light was ignored, the DNS method showed no bias in GPP on any timescale, and led to an underestimation of R_{above} about 20.4% (Fig. 10). In contrast, if the reduction in leaf respiration by light was ignored, the NNS method led to an overestimation of GPP about 4.7%, and an overestimation of R_{above} about 23.9% (Fig. 10).

4. Discussion

We developed a three-way flux-partitioning algorithm to partition NEE into R_{above}, R_{below}, and GPP. Our algorithm took advantage of the availability of continuous chamber-measured soil respiration and EC-measured NEE of CO_2, differential responses of GPP and respiration to environmental conditions, and the fact that R_{above} responds to air temperature measured above canopy while R_{below} responds to soil temperature and moisture. CO_2 flux partitioning algorithms have been widely used to partition the net ecosystem CO_2 exchange into two component fluxes, GPP and R_{eco} (Lasslop et al., 2010; Reichstein et al., 2005). This procedure is usually based on a semi-empirical model relating respiration to temperature (Lasslop et al., 2012). However, ecosystem respiratory fluxes consist of aboveground plant respiration, and belowground root and soil respiration, which are mainly driven by air temperature, and soil temperature and moisture, respectively (Barba et al., 2018; Järveoja et al., 2018). Soil temperature is always dampened with smaller variability compared to air temperature (Li et al., 2019), which contributed to a higher temperature sensitivity of R_{below} from soil temperature than that of R_{above} from air temperature in our results. Several studies have studied the time series of air temperature (Greco and Baldocchi, 1996; Valentini et al., 1996), soil temperature (Black et al., 1996; Goulden et al., 1996), and a weighted mean of soil and air temperature (Kutzbach et al., 2007; Lasslop et al., 2012) with respect to their ability to describe R_{eco}. However, there is currently no agreement as to which temperature is the most appropriate for modelling R_{eco} (Lasslop et al., 2012; Wohlfahrt and Galvagno, 2017). Our results showed that the temperature sensitivity of R_{eco} responded differently to air and soil temperature. Moreover, the

results of Wohlfahrt and Galvagno (2017) revealed that the phase shift between air and soil temperature yielded biased R_{eco} estimates, and the bias could be avoided by adopting a dual-source respiration model consisting of an above- and a belowground respiration source with corresponding driving temperatures. However, Wang et al. (2001) found that resolving the contribution of plant and soil respiration to R_{eco} was impossible due to a strong correlation between leaf and soil respiration parameters. Wohlfahrt et al. (2005a) reported that R_{above} and R_{below} parameters could be derived from measurements of R_{eco}, provided available data cover a wide range of fractional contributions of plants and soil to R_{eco}. Moreover, Oikawa et al. (2017) thought that R_{below} measurements can be combined with measurements of R_{above} and/or modeling to partition NEE**.** Therefore, different respiration source each driven by a corresponding temperature can be taken advantage of to partition NEE into R_{above}, R_{below}, and GPP.

The three-way CO_2 flux-partitioning algorithm provided an effective means of evaluating the temporal dynamics of aboveground plant respiration (R_{above}), belowground root and soil respiration (R_{below}), and gross primary production (GPP). Results of EC measurements presented here indicated that as plants took up CO_2 from the start of green-up (late April to early May) to the end of senescence (mid-to-late October) (Fig. 5), daily R_{above} and R_{below} also increased gradually at the start of the growing season and then decreased as the growing season progressed (Fig. 3). Meanwhile, at the growing season scale, the daily variations of NEE were most closely related to GPP rather than to R_{above} and R_{below}. These suggested that the seasonal rise and decline in photosynthesis and respiration of forest ecosystems corresponded closely with the timing of the phenological development and senescence (Järveoja et al., 2018). In addition, the seasonal dynamics of R_{above}, R_{below}, and GPP was likely related to the timing, frequency, and amount of rain events (Unger et al., 2009). For example, the significant drop in precipitation for August 2013 led to a gradual reduction in R_{below}, and the extreme precipitation events in July and October 2009 also suppressed R_{below} (Liu et al., 2020). In contrast to R_{below}, we found that R_{above} did not strongly respond to precipitation changes. Year 2012 was the driest of the last 10 years (Liu et al., 2020), and annual R_{below} in this year was lowest, but annual R_{above} did not decrease significantly (Fig. 4). Moreover, we found compelling evidence of nonlinear responses of soil respiration to soil moisture (Liu et al., 2020), while the variation of R_{above} with soil moisture was not obvious (data not shown). This indicates that there are other factors

such as temperature in addition to rain events that jointly regulate R_{above}. Meanwhile, GPP also responded positively to precipitation change, severe drought events in 2012 caused important reductions in GPP. Then there was a gradual increase of GPP in 2013 due to higher precipitation but R_{below} remained low, which reached normal values in 2014 (Fig. 4, 6). The seasonal and annual variability in estimated R_{above}, R_{below}, and GPP demonstrated the importance of long-term high-resolution time series when interpreting ecosystem data (van Gorsel et al., 2008).

Many studies have combined EC CO_2 flux partitioning results and soil respiration measurements to investigate the components, drivers and temporal dynamics of ecosystem respiration (Gaumont-Guay et al., 2006; Järveoja et al., 2018; Jassal et al., 2007; Rana et al., 2018; Suleau et al., 2011). However, there is still a lack of detailed knowledge on above- and belowground respiratory components with differing driving temperatures. One underlying reason is that the EC and chamber technique do not allow for quantifying the individual fluxes driven by different temperatures with a high temporal resolution. In this study, we provided year-round high temporal resolution estimate of R_{above} from the balance between the hourly NEE and R_{below} measurements. Our three-way CO_2 flux-partitioning results demonstrated that R_{above} and R_{below} accounted for 13.6-33.1% and 66.9-86.4% of the total R_{eco}, respectively, and the ratio varied with the seasons (Table 1). Our R_{below} to R_{eco} ratio was similar to data from Jassal et al. (2007), who found that R_{below}/R_{eco} varied between 52% in spring and 86% in winter. Soil respiration was a large source of total ecosystem respiration and respiration from aboveground sources was only a small component of R_{eco} (Wang et al., 2010). Consequently, interannual variation of R_{eco} at the site was controlled mostly by interannual variation of R_{below}. The ratio of R_{above} and R_{below} to GPP could be used to evaluate the relative contribution of component respiration and photosynthesis to the total ecosystem carbon exchange (Dyukarev, 2017). Mean annual R_{above}, R_{below}, and GPP were 243, 806, and 1170 g C m^{-2}, respectively, with annual R_{eco} accounting for 89.6% of GPP, of which 68.8% was lost as belowground root and soil respiration and 20.8% lost as aboveground plant respiration, and leaving only 10% of autochthonous carbon fixation in the ecosystem (Fig 4, 6). Our results were similar to data from Jassal et al. (2007), who found that about 54% of carbon fixed in GPP was lost as autotrophic respiration and the other 32% was lost in the decomposition of soil organic matter and

litter. The studied ecosystem is a sink of carbon according to modelling and observation results.

This study compared EC-derived nighttime NEE to nighttime soil respiration measured with automated chambers. On average, EC-measured NEE_{night} were generally lower than chamber-measured $R_{below,night}$ when summer and winter windspeed below 2.66 and 1.77 m s^{-1}, respectively (Fig. 1). This was consistent with other studies (Oechel et al., 1998; Wang et al., 2010). Several studies have reported lower estimates of NEE_{night} derived from EC measurements (Bolstad et al., 2004; Gaumont-Guay et al., 2006; Griffis et al., 2004; Lavigne et al., 1997; Miyama et al., 2006), while others have reported good agreement between the two techniques during periods of canopy absence (Myklebust et al., 2008; Reth et al., 2005). Although chamber measurements are not free of uncertainty (Gaumont-Guay et al., 2006), previous comparisons between chamber- and EC-based estimates have provided evidence that EC method likely produces biased estimates of forest CO_2 fluxes (Griffis et al., 2003; Khomik et al., 2010; Wang et al., 2017), and underestimated NEE_{night} could be attributed to CO_2 accumulation near the surface in stable or calm conditions (Aubinet et al., 2001; Loescher et al., 2006) which cannot be adequately corrected for by a profiling system at a single location. This supported Law et al. (1999) and Myklebust et al. (2008) who assumed that with higher u_* threshold, greater mixing of the canopy air would result in more accurate estimates of NEE_{night} (Ohkubo et al., 2007; Wang et al., 2010). In many studies, a correction was applied to EC-measured NEE_{night} to address the underestimation of R_{eco} during atmospherically stable nights (Janssens et al., 2001; Ohkubo et al., 2007). For example, van Gorsel et al. (2008) used the maximum NEE in the early evening to build a temperature response function for nighttime R_{eco}. Janssens et al. (2001) replaced NEE_{night} with a value computed from a temperature response function when u_* falls below a threshold. The method most widely used to correct for flux underestimation during stable nights was applied in this study. It consists of replacing the flux measured during stable nighttime periods by a value simulated with a temperature response function derived during well-mixed nighttime conditions.

Estimates of R_{above}, R_{below}, and GPP derived from simplified NEE models are associated with large uncertainties (Janssens et al., 2001). One cause of this is failure to incorporate the light inhibition of foliar respiration (Heskel et al., 2013). $R_{eco,day}$ is likely to differ from $R_{eco,night}$ because of light-induced inhibition of leaf respiration

(Janssens et al., 2001). The extrapolation of R_{eco} between day and night conditions may result in over- or underestimation in both canopy respiration and ecosystem carbon fluxes (Crous et al., 2012; Heskel and Tang, 2018; Kroner and Way, 2016). Keenan et al. (2019) developed a flux partitioning algorithm that could detect an apparent ecosystem-scale inhibition of daytime respiration. However, the Kok effect could only inhibit canopy respiration but not soil plus root respiratory fluxes (Tcherkez et al., 2017; Wohlfahrt et al., 2005b). Incorporating soil respiration into the light inhibition of foliar respiration may aggravate photoinhibition effect and thus under- or overestimate inhibition biases in both canopy respiration and GPP. Using the flux partitioning algorithms of Keenan et al. (2019), we calculated the estimation bias in R_{above} and GPP due to the light inhibition of leaf respiration, and the bias we reported was in line with Sun et al. (2014) who showed that canopy respiration and GPP were overestimated by approximately 20.4% and 4.6%, respectively. These results provide valuable insight on how variation in light inhibition of respiration affects the prediction of aboveground carbon balance. Further, future research should consider partitioning R_{eco} into canopy leaf and residual (trunk and soil) respiration, and incorporating light inhibition of respiration into NEE models to accurately predict rates of carbon exchange at canopy level (Crous et al., 2012).

5. Conclusion

This paper developed a three-way CO_2 flux-partitioning algorithm to decompose NEE into R_{above}, R_{below}, and GPP. Using continuous chamber-measured soil respiration and EC-measured NEE of CO_2, we estimated R_{above}, R_{below}, and GPP over a decade for a deciduous forest in the US Midwest. We found that R_{above} and R_{below} accounted for 13.6-33.1% and 66.9-86.4% of the total R_{eco}, respectively and the percentages varied with the seasons. Mean annual R_{above}, R_{below}, and GPP were 243, 806, and 1170 g C m^{-2}, respectively, with annual R_{eco} accounting for 89.6% of GPP, of which 68.8% was lost as R_{below} and 20.8% lost as R_{above}, leaving only 10% of carbon fixation in ecosystems. The DNS method underestimated annual R_{above} (about 20.4%), and the NNS method overestimated R_{above} (about 23.9%) and GPP (about 4.7%). We found that belowground respiration has much greater sensitivity to temperature than aboveground respiration does. Our findings suggest that accounting for the respiratory heterogeneity in the

various ecosystem components is crucial for understanding and predicting ecosystem carbon balance.

Acknowledgements

This research was supported by the Natural Science Foundation of Hebei Province (D2021503009), the "Strategic Priority Research Program" of the Chinese Academy of Sciences (XDA28020303, XDA26040103), the National Key Research and Development Program of China (2016YFC0500802) and Visiting Scholars Program of Chinese Academy of Sciences. LG is supported by the U.S. Department of Energy (DOE), Office of Science, Biological and Environmental Research Program. ORNL is managed by UT-Battelle, LLC, for DOE under contract DE-AC05-00OR22725.

References

Aubinet, M., Chermanne, B., Vandenhaute, M., Longdoz, B., Yernaux, M. and Laitat, E., 2001. Long term carbon dioxide exchange above a mixed forest in the Belgian Ardennes. Agricultural and Forest Meteorology, 108(4): 293-315.

Barba, J., Cueva, A., Bahn, M., Barron-Gaffordd, G.A., Bond-Lamberty, B., Hanson, P.J., Jaimes, A., Kulmala, L., Pumpanen, J., Scott, R.L., Wohlfahrt, G. and Vargas, R., 2018. Comparing ecosystem and soil respiration: Review and key challenges of tower-based and soil measurements. Agricultural and Forest Meteorology, 249: 434-443.

Black, T.A., DenHartog, G., Neumann, H.H., Blanken, P.D., Yang, P.C., Russell, C., Nesic, Z., Lee, X., Chen, S.G., Staebler, R. and Novak, M.D., 1996. Annual cycles of water vapour and carbon dioxide fluxes in and above a boreal aspen forest. Global Change Biology, 2(3): 219-229.

Bolstad, P.V., Davis, K.J., Martin, J., Cook, B.D. and Wang, W., 2004. Component and whole-system respiration fluxes in northern deciduous forests. Tree Physiology, 24(5): 493-504.

Brito, P., Soledad Jimenez, M., Morales, D. and Wieser, G., 2013. Assessment of ecosystem CO_2 efflux and its components in a Pinus canariensis forest at the treeline. Trees-Structure and Function, 27(4): 999-1009.

Buckley, T.N., Vice, H. and Adams, M.A., 2017. The Kok effect in *Vicia faba* cannot be explained solely by changes in chloroplastic CO_2 concentration. New

Phytologist, 216(4): 1064-1071.

Crous, K.Y., Zaragoza-Castells, J., Ellsworth, D.S., Duursma, R.A., Loew, M., Tissue, D.T. and Atkin, O.K., 2012. Light inhibition of leaf respiration in field-grown *Eucalyptus saligna* in whole-tree chambers under elevated atmospheric CO_2 and summer drought. Plant Cell and Environment, 35(5): 966-981.

Dyukarev, E.A., 2017. Partitioning of net ecosystem exchange using chamber measurements data from bare soil and vegetated sites. Agricultural and Forest Meteorology, 239: 236-248.

Gaumont-Guay, D., Black, T.A., Griffis, T.J., Barr, A.G., Morgenstern, K., Jassal, R.S. and Nesic, Z., 2006. Influence of temperature and drought on seasonal and interannual variations of soil, bole and ecosystem respiration in a boreal aspen stand. Agricultural and Forest Meteorology, 140(1): 203-219.

Gilmanov, T.G., Wylie, B.K., Tieszen, L.L., Meyers, T.P., Baron, V.S., Bernacchi, C.J., Billesbach, D.P., Burba, G.G., Fischer, M.L., Glenn, A.J., Hanan, N.P., Hatfield, J.L., Heuer, M.W., Hollinger, S.E., Howard, D.M., Matamala, R., Prueger, J.H., Tenuta, M. and Young, D.G., 2013. CO_2 uptake and ecophysiological parameters of the grain crops of midcontinent North America: Estimates from flux tower measurements. Agriculture, Ecosystems & Environment, 164: 162-175.

Goulden, M.L., Munger, J.W., Fan, S.M., Daube, B.C. and Wofsy, S.C., 1996. Measurements of carbon sequestration by long-term eddy covariance: Methods and a critical evaluation of accuracy. Global Change Biology, 2(3): 169-182.

Greco, S. and Baldocchi, D.D., 1996. Seasonal variations of CO_2 and water vapour exchange rates over a temperate deciduous forest. Global Change Biology, 2(3): 183-197.

Griffis, T.J., Black, T.A., Gaumont-Guay, D., Drewitt, G.B., Nesic, Z., Barr, A.G., Morgenstern, K. and Kljun, N., 2004. Seasonal variation and partitioning of ecosystem respiration in a southern boreal aspen forest. Agricultural and Forest Meteorology, 125(3-4): 207-223.

Griffis, T.J., Black, T.A., Morgenstern, K., Barr, A.G., Nesic, Z., Drewitt, G.B., Gaumont-Guay, D. and McCaughey, J.H., 2003. Ecophysiological controls on the carbon balances of three southern boreal forests. Agricultural and Forest Meteorology, 117(1-2): 53-71.

Gu, L., Falge, E.M., Boden, T., Baldocchi, D.D., Black, T.A., Saleska, S.R., Suni, T., Verma, S.B., Vesala, T., Wofsy, S.C. and Xu, L., 2005. Objective threshold determination for nighttime eddy flux filtering. Agricultural and Forest Meteorology, 128(3): 179-197.

Gu, L., Massman, W.J., Leuning, R., Pallardy, S.G., Meyers, T., Hanson, P.J., Riggs, J.S., Hosman, K.P. and Yang, B., 2012. The fundamental equation of eddy covariance and its application in flux measurements. Agricultural and Forest Meteorology, 152: 135-148.

Gu, L., Meyers, T., Pallardy, S.G., Hanson, P.J., Yang, B., Heuer, M., Hosman, K.P., Riggs, J.S., Sluss, D. and Wullschleger, S.D., 2006. Direct and indirect effects of atmospheric conditions and soil moisture on surface energy partitioning revealed by a prolonged drought at a temperate forest site. Journal of Geophysical Research: Atmospheres, 111(D16): doi:10.1029/2006jd007161.

Gu, L., Pallardy, S.G., Yang, B., Hosman, K.P., Mao, J., Ricciuto, D., Shi, X. and Sun, Y., 2016. Testing a land model in ecosystem functional space via a comparison of observed and modeled ecosystem flux responses to precipitation regimes and associated stresses in a Central U.S. forest. Journal of Geophysical Research: Biogeosciences, 121(7): 1884-1902.

Heskel, M.A., Atkin, O.K., Turnbull, M.H. and Griffin, K.L., 2013. Bringing the Kok effect to light: A review on the integration of daytime respiration and net ecosystem exchange. Ecosphere, 4(8): doi: 10.1890/ES13-00120.1.

Heskel, M.A. and Tang, J., 2018. Environmental controls on light inhibition of respiration and leaf and canopy daytime carbon exchange in a temperate deciduous forest. Tree Physiology, 38(12): 1886-1902.

Hutyra, L.R., Munger, J.W., Hammond-Pyle, E., Saleska, S.R., Restrepo-Coupe, N., Daube, B.C., de Camargo, P.B. and Wofsy, S.C., 2008. Resolving systematic errors in estimates of net ecosystem exchange of CO_2 and ecosystem respiration in a tropical forest biome. Agricultural and Forest Meteorology, 148(8-9): 1266-1279.

Janssens, I.A., Lankreijer, H., Matteucci, G., Kowalski, A.S., Buchmann, N., Epron, D., Pilegaard, K., Kutsch, W., Longdoz, B., Grunwald, T., Montagnani, L., Dore, S., Rebmann, C., Moors, E.J., Grelle, A., Rannik, U., Morgenstern, K., Oltchev, S., Clement, R., Gudmundsson, J., Minerbi, S., Berbigier, P., Ibrom, A.,

548 Moncrieff, J., Aubinet, M., Bernhofer, C., Jensen, N.O., Vesala, T., Granier, A.,
549 Schulze, E.D., Lindroth, A., Dolman, A.J., Jarvis, P.G., Ceulemans, R. and
550 Valentini, R., 2001. Productivity overshadows temperature in determining soil
551 and ecosystem respiration across European forests. Global Change Biology,
552 7(3): 269-278.
553 Järveoja, J., Nilsson, M.B., Gažovič, M., Crill, P.M. and Peichl, M., 2018. Partitioning
554 of the net CO_2 exchange using an automated chamber system reveals plant
555 phenology as key control of production and respiration fluxes in a boreal
556 peatland. Global Change Biology, 24(8): 3436-3451.
557 Jassal, R.S., Black, T.A., Cai, T., Morgenstern, K., Li, Z., Gaumont-Guay, D. and Nesic,
558 Z., 2007. Components of ecosystem respiration and an estimate of net primary
559 productivity of an intermediate-aged Douglas-fir stand. Agricultural and Forest
560 Meteorology, 144(1-2): 44-57.
561 Keenan, T.F., Migliavacca, M., Papale, D., Baldocchi, D., Reichstein, M., Torn, M. and
562 Wutzler, T., 2019. Widespread inhibition of daytime ecosystem respiration.
563 Nature Ecology & Evolution, 3(3): doi: 10.1038/s41559-019-0809-2.
564 Khomik, M., Arain, M.A., Brodeur, J.J., Peichl, M., Restrepo-Coupe, N. and McLaren,
565 J.D., 2010. Relative contributions of soil, foliar, and woody tissue respiration to
566 total ecosystem respiration in four pine forests of different ages. Journal of
567 Geophysical Research-Biogeosciences, 115: doi: 10.1029/2009JG001089.
568 Kok, B., 1948. A critical consideration of quantum yield of *Chlorella*-photosynthesis.
569 Enzymologia, 13: 1-56.
570 Kok, B., 1949. On the interrelation of respiration and photosynthesis in green plates.
571 Biochimica Et Biophysica Acta, 3(5-6): 625-631.
572 Kroner, Y. and Way, D.A., 2016. Carbon fluxes acclimate more strongly to elevated
573 growth temperatures than to elevated CO_2 concentrations in a northern conifer.
574 Global Change Biology, 22(8): 2913-2928.
575 Kruse, J., Rennenberg, H. and Adams, M.A., 2011. Steps towards a mechanistic
576 understanding of respiratory temperature responses. New Phytologist, 189(3):
577 659-677.
578 Kutzbach, L., Wille, C. and Pfeiffer, E.M., 2007. The exchange of carbon dioxide
579 between wet arctic tundra and the atmosphere at the Lena River Delta, Northern
580 Siberia. Biogeosciences, 4(5): 869-890.

Lasslop, G., Migliavacca, M., Bohrer, G., Reichstein, M., Bahn, M., Ibrom, A., Jacobs, C., Kolari, P., Papale, D., Vesala, T., Wohlfahrt, G. and Cescatti, A., 2012. On the choice of the driving temperature for eddy-covariance carbon dioxide flux partitioning. Biogeosciences, 9(12): 5243-5259.

Lasslop, G., Reichstein, M., Papale, D., Richardson, A.D., Arneth, A., Barr, A., Stoy, P. and Wohlfahrt, G., 2010. Separation of net ecosystem exchange into assimilation and respiration using a light response curve approach: critical issues and global evaluation. Global Change Biology, 16(1): 187-208.

Lavigne, M.B., Ryan, M.G., Anderson, D.E., Baldocchi, D.D., Crill, P.M., Fitzjarrald, D.R., Goulden, M.L., Gower, S.T., Massheder, J.M., McCaughey, J.H., Rayment, M. and Striegl, R.G., 1997. Comparing nocturnal eddy covariance measurements to estimates of ecosystem respiration made by scaling chamber measurements at six coniferous boreal sites. Journal of Geophysical Research-Atmospheres, 102(D24): 28977-28985.

Law, B.E., Baldocchi, D.D. and Anthoni, P.M., 1999. Below-canopy and soil CO_2 fluxes in a ponderosa pine forest. Agricultural and Forest Meteorology, 94(3-4): 171-188.

Li, Q., Song, X., Chang, S.X., Peng, C., Xiao, W., Zhang, J., Xiang, W., Li, Y. and Wang, W., 2019. Nitrogen depositions increase soil respiration and decrease temperature sensitivity in a Moso bamboo forest. Agricultural and Forest Meteorology, 268: 48-54.

Liu, X., Liang, J. and Gu, L., 2020. Photosynthetic and environmental regulations of the dynamics of soil respiration in a forest ecosystem revealed by analyses of decadal time series. Agricultural and Forest Meteorology, 282: doi: 10.1016/j.agrformet.2019.107863.

Lloyd, J. and Taylor, J.A., 1994. On the temperature-dependence of soil respiration. Functional Ecology, 8(3): 315-323.

Loescher, H.W., Law, B.E., Mahrt, L., Hollinger, D.Y., Campbell, J. and Wofsy, S.C., 2006. Uncertainties in, and interpretation of, carbon flux estimates using the eddy covariance technique. Journal of Geophysical Research-Atmospheres, 111(D21): doi: 10.1029/2005JD006932.

Mauder, M. and Foken, T., 2011. Documentation and Instruction Manual of the Eddy Covariance Software Package TK2. Arbeitsergebnisse, Universität Bayreuth,

614 Abteilung Mikrometeorologie, ISSN 1614-8916, 46.
615 Miao, G., Noormets, A., Domec, J.-C., Fuentes, M., Trettin, C.C., Sun, G., McNulty,
616 S.G. and King, J.S., 2017. Hydrology and microtopography control carbon
617 dynamics in wetlands: Implications in partitioning ecosystem respiration in a
618 coastal plain forested wetland. Agricultural and Forest Meteorology, 247: 343-
619 355.
620 Miyama, T., Kominami, Y., Tamai, K., Goto, Y., Kawahara, T., Jomura, M. and
621 Dannoura, M., 2006. Components and seasonal variation of night-time total
622 ecosystem respiration in a Japanese broad-leaved secondary forest. Tellus
623 Series B-Chemical and Physical Meteorology, 58(5): 550-559.
624 Moore, B., III, Crowell, S.M.R., Rayner, P.J., Kumer, J., O'Dell, C.W., O'Brien, D.,
625 Utembe, S., Polonsky, I., Schimel, D. and Lemen, J., 2018. The Potential of the
626 Geostationary Carbon Cycle Observatory (GeoCarb) to Provide Multi-scale
627 Constraints on the Carbon Cycle in the Americas. Frontiers in Environmental
628 Science, 6: doi: 10.3389/fenvs.2018.00109.
629 Myklebust, M.C., Hipps, L.E. and Ryel, R.J., 2008. Comparison of eddy covariance,
630 chamber, and gradient methods of measuring soil CO_2 efflux in an annual semi-
631 arid grass, Bromus tectorum. Agricultural and Forest Meteorology, 148(11):
632 1894-1907.
633 Oechel, W.C., Vourlitis, G.L., Brooks, S., Crawford, T.L. and Dumas, E., 1998.
634 Intercomparison among chamber, tower, and aircraft net CO_2 and energy fluxes
635 measured during the Arctic System Science Land-Atmosphere-Ice Interactions
636 (ARCSS-LAII) Flux Study. Journal of Geophysical Research-Atmospheres,
637 103(D22): 28993-29003.
638 Ogee, J., Peylin, P., Cuntz, M., Bariac, T., Brunet, Y., Berbigier, P., Richard, P. and
639 Ciais, P., 2004. Partitioning net ecosystem carbon exchange into net
640 assimilation and respiration with canopy-scale isotopic measurements: An error
641 propagation analysis with $^{13}CO_2$ and $CO^{18}O$ data. Global Biogeochemical
642 Cycles, 18(2): doi: 10.1029/2003GB002166.
643 Ohkubo, S., Kosugi, Y., Takanashi, S., Mitani, T. and Tani, M., 2007. Comparison of
644 the eddy covariance and automated closed chamber methods for evaluating
645 nocturnal CO_2 exchange in a Japanese cypress forest. Agricultural and Forest
646 Meteorology, 142(1): 50-65.

Oikawa, P.Y., Sturtevant, C., Knox, S.H., Verfaillie, J., Huang, Y.W. and Baldocchi, D.D., 2017. Revisiting the partitioning of net ecosystem exchange of CO_2 into photosynthesis and respiration with simultaneous flux measurements of $^{13}CO_2$ and CO_2, soil respiration and a biophysical model, CANVEG. Agricultural and Forest Meteorology, 234: 149-163.

Paul-Limoges, E., Wolf, S., Eugster, W., Hoertnagl, L. and Buchmann, N., 2017. Below-canopy contributions to ecosystem CO_2 fluxes in a temperate mixed forest in Switzerland. Agricultural and Forest Meteorology, 247: 582-596.

Raj, R., Hamm, N.A.S., van der Tol, C. and Stein, A., 2016. Uncertainty analysis of gross primary production partitioned from net ecosystem exchange measurements. Biogeosciences, 13(5): 1409-1422.

Rana, G., Palatella, L., Scanlon, T.M., Martinelli, N. and Ferrara, R.M., 2018. CO_2 and H_2O flux partitioning in a Mediterranean cropping system. Agricultural and Forest Meteorology, 260: 118-130.

Reichstein, M., Falge, E., Baldocchi, D., Papale, D., Aubinet, M., Berbigier, P., Bernhofer, C., Buchmann, N., Gilmanov, T., Granier, A., Grünwald, T., Havránková, K., Ilvesniemi, H., Janous, D., Knohl, A., Laurila, T., Lohila, A., Loustau, D., Matteucci, G., Meyers, T., Miglietta, F., Ourcival, J.-M., Pumpanen, J., Rambal, S., Rotenberg, E., Sanz, M., Tenhunen, J., Seufert, G., Vaccari, F., Vesala, T., Yakir, D. and Valentini, R., 2005. On the separation of net ecosystem exchange into assimilation and ecosystem respiration: review and improved algorithm. Global Change Biology, 11(9): 1424-1439.

Reth, S., Gockede, M. and Falge, E., 2005. CO_2 efflux from agricultural soils in Eastern Germany - comparison of a closed chamber system with eddy covariance measurements. Theoretical and Applied Climatology, 80(2-4): 105-120.

Suleau, M., Moureaux, C., Dufranne, D., Buysse, P., Bodson, B., Destain, J.-P., Heinesch, B., Debacq, A. and Aubinet, M., 2011. Respiration of three Belgian crops: Partitioning of total ecosystem respiration in its heterotrophic, above- and below-ground autotrophic components. Agricultural and Forest Meteorology, 151(5): 633-643.

Sun, J., Wu, J., Guan, D., Yao, F., Yuan, F., Wang, A. and Jin, C., 2014. Estimating daytime ecosystem respiration to improve estimates of gross primary production of a temperate forest. Plos One, 9(11): doi: 10.1371/journal.pone.0113512.

Tcherkez, G., Gauthier, P., Buckley, T.N., Busch, F.A., Barbour, M.M., Bruhn, D., Heskel, M.A., Gong, X.Y., Crous, K.Y., Griffin, K., Way, D., Turnbull, M., Adams, M.A., Atkin, O.K., Farquhar, G.D. and Cornic, G., 2017. Leaf day respiration: low CO_2 flux but high significance for metabolism and carbon balance. New Phytologist, 216(4): 986-1001.

Tcherkez, G., Mahé, A., Gauthier, P., Mauve, C., Gout, E., Bligny, R., Cornic, G. and Hodges, M., 2009. In Folio Respiratory Fluxomics Revealed by ^{13}C Isotopic Labeling and H/D Isotope Effects Highlight the Noncyclic Nature of the Tricarboxylic Acid "Cycle" in Illuminated Leaves. Plant Physiology, 151(2): 620-630.

Unger, S., Maguas, C., Pereira, J.S., Aires, L.M., David, T.S. and Werner, C., 2009. Partitioning carbon fluxes in a Mediterranean oak forest to disentangle changes in ecosystem sink strength during drought. Agricultural and Forest Meteorology, 149(6-7): 949-961.

Valentini, R., DeAngelis, P., Matteucci, G., Monaco, R., Dore, S. and Mugnozza, G.E.S., 1996. Seasonal net carbon dioxide exchange of a beech forest with the atmosphere. Global Change Biology, 2(3): 199-207.

van Gorsel, E., Leuning, R., Cleugh, H.A., Keith, H., Kirschbaum, M.U.F. and Suni, T., 2008. Application of an alternative method to derive reliable estimates of nighttime respiration from eddy covariance measurements in moderately complex topography. Agricultural and Forest Meteorology, 148(6): 1174-1180.

Wang, M., Guan, D.-X., Han, S.-J. and Wu, J.-L., 2010. Comparison of eddy covariance and chamber-based methods for measuring CO_2 flux in a temperate mixed forest. Tree Physiology, 30(1): 149-163.

Wang, X., Wang, C. and Bond-Lamberty, B., 2017. Quantifying and reducing the differences in forest CO_2-fluxes estimated by eddy covariance, biometric and chamber methods: A global synthesis. Agricultural and Forest Meteorology, 247: 93-103.

Wang, Y.P., Leuning, R., Cleugh, H.A. and Coppin, P.A., 2001. Parameter estimation in surface exchange models using nonlinear inversion: how many parameters can we estimate and which measurements are most useful? Global Change Biology, 7(5): 495-510.

Wohlfahrt, G., Anfang, C., Bahn, M., Haslwanter, A., Newesely, C., Schmitt, M.,

Drosler, M., Pfadenhauer, J. and Cernusca, A., 2005a. Quantifying nighttime ecosystem respiration of a meadow using eddy covariance, chambers and modelling. Agricultural and Forest Meteorology, 128(3-4): 141-162.

Wohlfahrt, G., Bahn, M., Haslwanter, A., Newesely, C. and Cernusca, A., 2005b. Estimation of daytime ecosystem respiration to determine gross primary production of a mountain meadow. Agricultural and Forest Meteorology, 130(1-2): 13-25.

Wohlfahrt, G. and Galvagno, M., 2017. Revisiting the choice of the driving temperature for eddy covariance CO_2 flux partitioning. Agricultural and Forest Meteorology, 237: 135-142.

Xu, L.K. and Baldocchi, D.D., 2004. Seasonal variation in carbon dioxide exchange over a Mediterranean annual grassland in California. Agricultural and Forest Meteorology, 123(1-2): 79-96.

Yang, B., Pallardy, S.G., Meyers, T.P., Gu, L.-H., Hanson, P.J., Wullschleger, S.D., Heuer, M., Hosman, K.P., Riggs, J.S. and Sluss, D.W., 2010. Environmental controls on water use efficiency during severe drought in an Ozark Forest in Missouri, USA. Global Change Biology, 16(8): 2252-2271.

Young, F.J., Radatz, C.A. and Marshall, C.A., 2001. Soil Survey of Boone County, Missouri. United States Department of Agriculture, Natural Resources Conservation Service.

Figure legends

Fig. 1 The difference between NEE_{night} and $R_{below,night}$ at low windspeed during the (a) growing and (b) non-growing season. NEE_{night} is the nighttime NEE; $R_{below,night}$ is the nighttime soil respiration; NEE_{night} and $R_{below,night}$ are half hourly data, and the difference between NEE_{night} and $R_{below,night}$ is the average within a bin of windspeed.

Fig. 2 Seasonal variability of NEE. NEE is daily total.

Fig. 3 Seasonal variability of above- (R_{above}) and belowground respiration (R_{below}). R_{above} and R_{below} are daily total. $R_{above\text{-}DNS}$: estimated aboveground respiration using daytime NEE and soil respiration (DNS) method; $R_{above\text{-}NNS}$: estimated aboveground respiration using nighttime NEE and soil respiration (NNS) method; R_{below}: belowground respiration.

Fig. 4 Annual above- (R_{above}) and belowground respiration (R_{below}) from 2006 to 2015. $R_{above\text{-}DNS}$: estimated aboveground respiration using daytime NEE and soil respiration (DNS) method; $R_{above\text{-}NNS}$: estimated aboveground respiration using nighttime NEE and soil respiration (NNS) method; R_{below}: belowground respiration.

Fig. 5 Seasonal variability of gross primary production (GPP). GPP is daily total. GPP_{DNS}: estimated gross primary production using daytime NEE and soil respiration (DNS) method; GPP_{NNS}: estimated gross primary production using nighttime NEE and soil respiration (NNS) method.

Fig. 6 Annual gross primary production (GPP) from 2006 to 2015. GPP_{DNS}: estimated gross primary production using daytime NEE and soil respiration (DNS) method; GPP_{NNS}: estimated gross primary production using nighttime NEE and soil respiration (NNS) method.

Fig. 7 Relationships of aboveground respiration (R_{above}) with air temperature, and belowground respiration (R_{below}) with soil temperature. R_{above} and R_{below} are half hourly data. R_{above}: estimated aboveground respiration using daytime NEE and soil respiration (DNS) method; R_{below}: belowground respiration.

Fig. 8 Relationships of half hourly ecosystem respiration (R_{eco}) with air and soil temperature. R_{eco}: estimated ecosystem respiration using daytime NEE and soil

763 respiration (DNS) method; R_{aeco}: air temperature sensitivity of ecosystem respiration;
764 R_{seco}: soil temperature sensitivity of ecosystem respiration.
765 Fig. 9 Seasonal cycles of reference respiration (R_{ref}) inferred from both daytime and
766 nighttime data. R_{ref} is monthly average. $R_{ref,day}$: estimated reference respiration by
767 daytime data; $R_{ref,night}$: estimated reference respiration by nighttime data.
768 Fig. 10 Relative biases in estimates of gross primary production (GPP) and
769 aboveground respiration (R_{above}). $R_{above\text{-}DNS}$ and GPP_{DNS}: estimated aboveground
770 respiration and gross primary production using daytime NEE and soil respiration (DNS)
771 method; $R_{above\text{-}NNS}$ and GPP_{NNS}: estimated aboveground respiration and gross primary
772 production using nighttime NEE and soil respiration (NNS) method.

773 Fig. 1

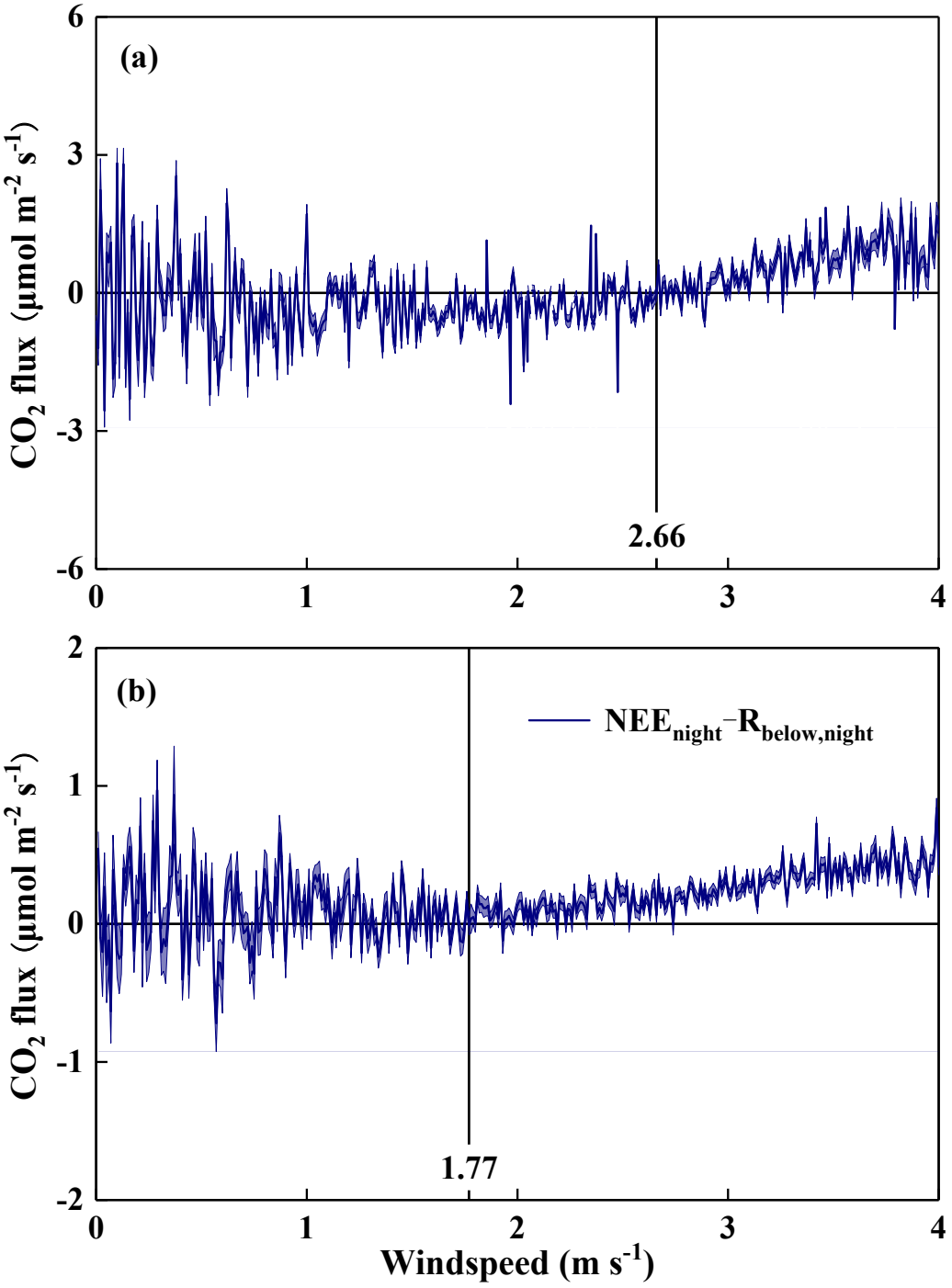
(a)
CO_2 flux (μmol m^{-2} s^{-1})
2.66
(b)
NEE_{night}–$R_{below,night}$
1.77
Windspeed (m s^{-1})

774

775 Fig. 2

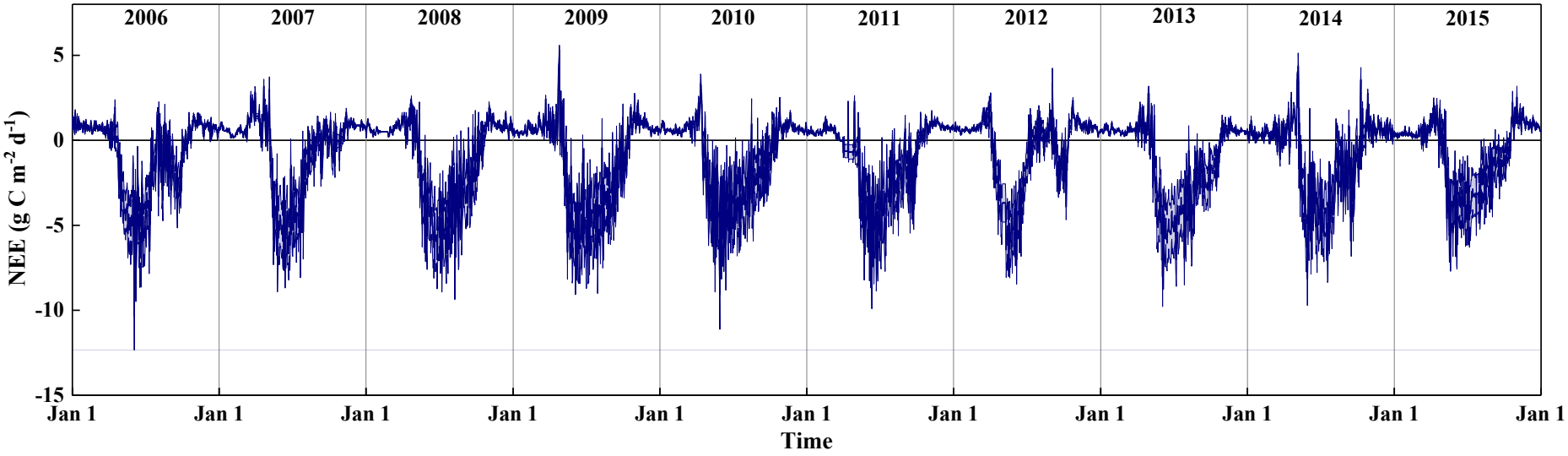
2006
2007
2008
2009
2010
2011
2012
2013
2014
2015
5
0
-5
-10
-15
NEE (g C m-2 d-1)
Jan 1
Jan 1
Jan 1
Jan 1
Jan 1
Jan 1
Jan 1
Jan 1
Jan 1
Jan 1
Jan 1
Time

776

777 Fig. 3

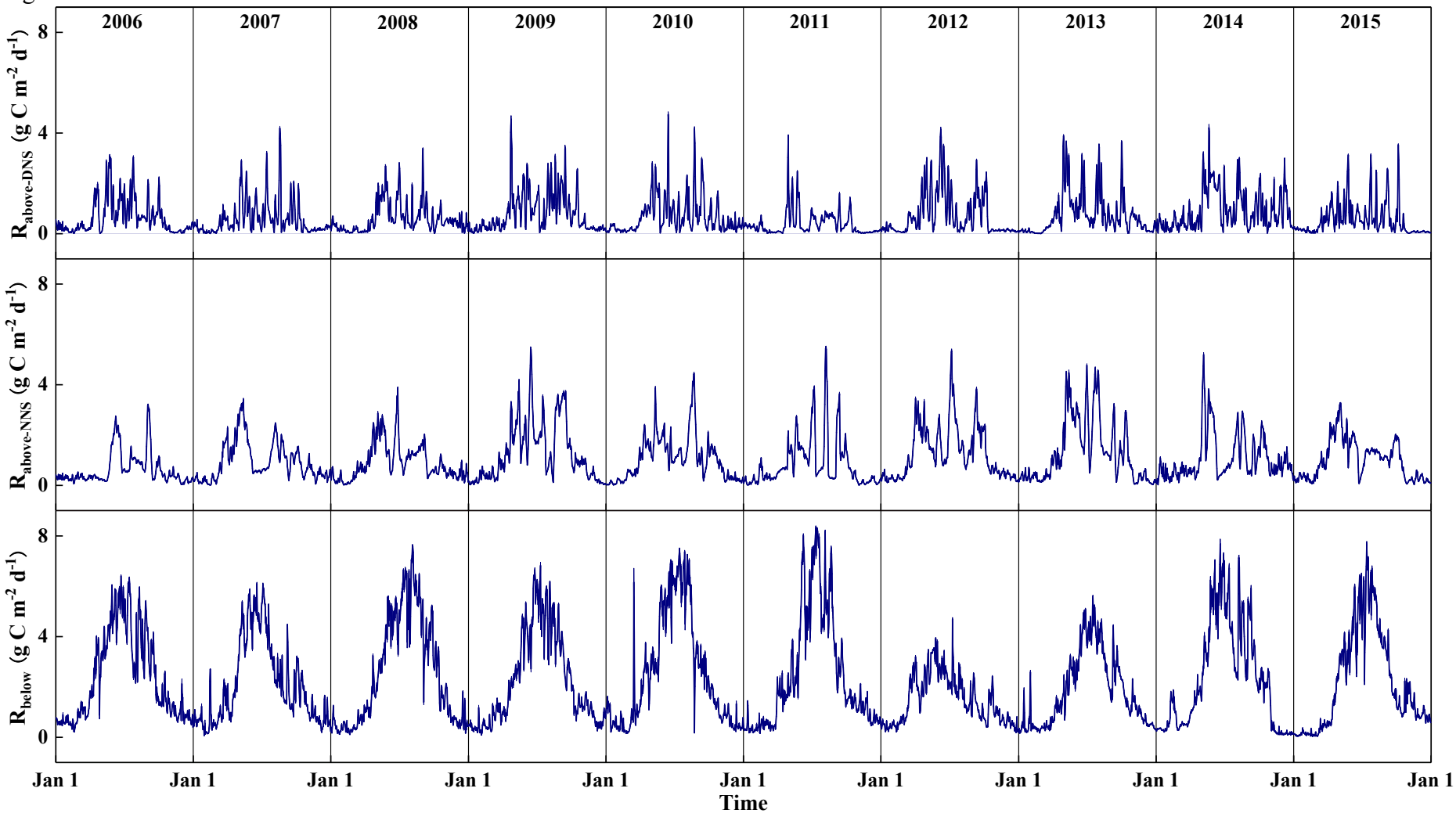
2006
2007
2008
2009
2010
2011
2012
2013
2014
2015
$R_{above\text{-}DNS}$ (g C m^{-2} d^{-1})
$R_{above\text{-}NNS}$ (g C m^{-2} d^{-1})
R_{below} (g C m^{-2} d^{-1})
0
4
8
Jan 1
Time

778

779 Fig. 4

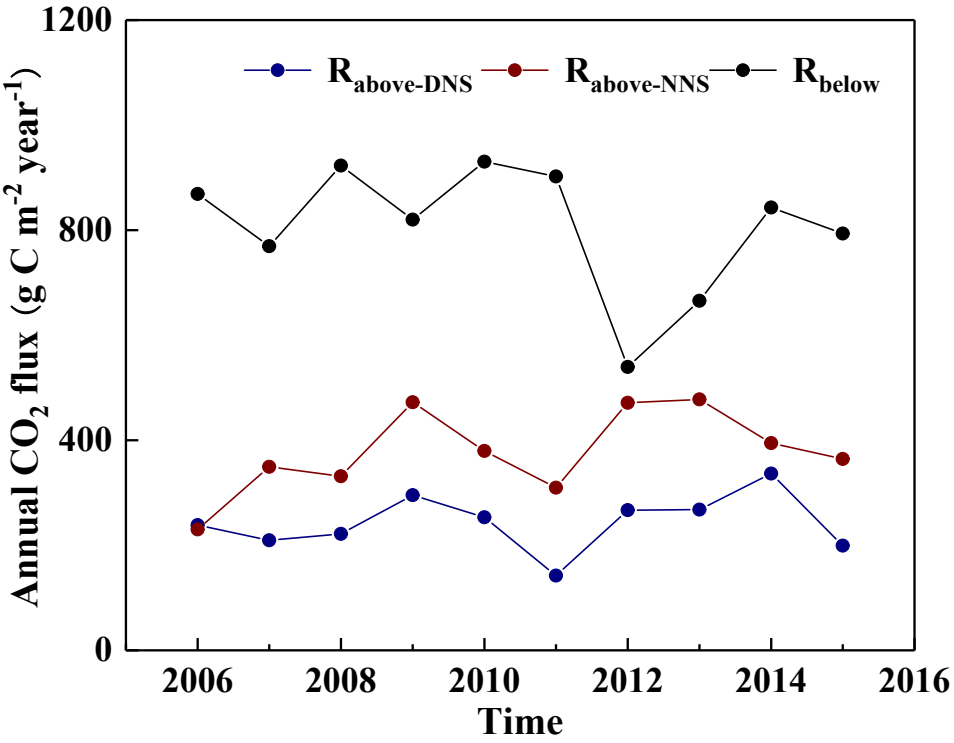
1200
800
400
0
Annual CO_2 flux (g C m^{-2} $year^{-1}$)
$R_{above-DNS}$
$R_{above-NNS}$
R_{below}
2006
2008
2010
2012
2014
2016
Time

780

781 Fig. 5

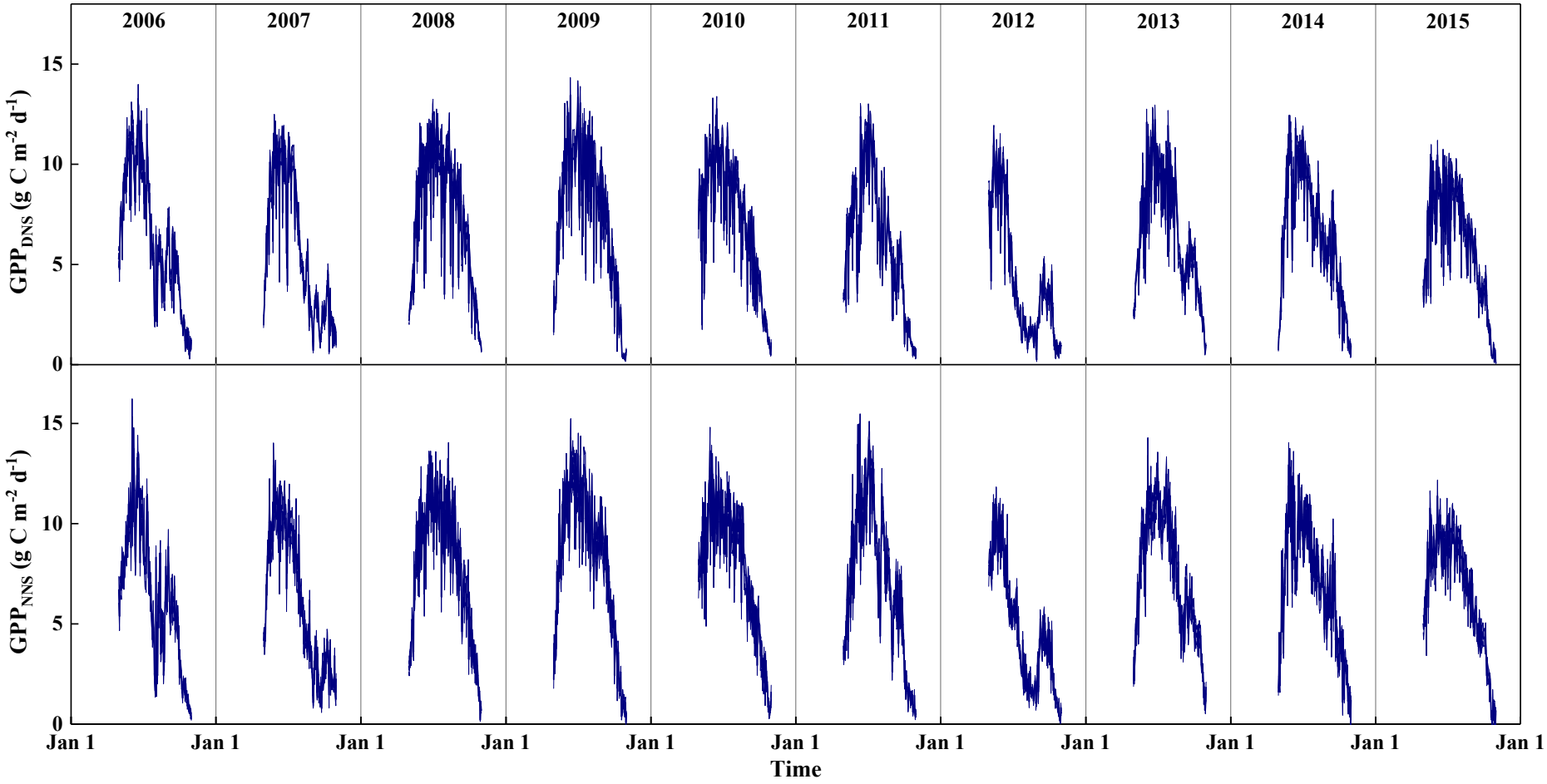
2006
2007
2008
2009
2010
2011
2012
2013
2014
2015
GPP$_{DNS}$ (g C m^{-2} d^{-1})
GPP$_{NNS}$ (g C m^{-2} d^{-1})
0
5
10
15
Jan 1
Time

782

783 Fig. 6

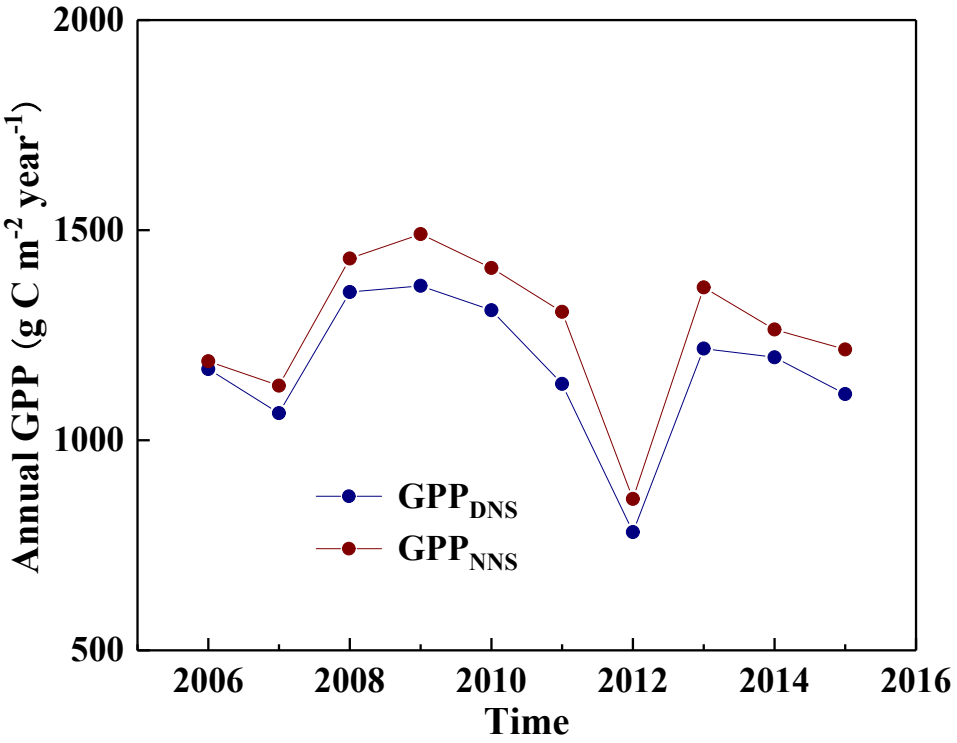
2000
1500
1000
500
Annual GPP (g C m-2 year-1)
2006
2008
2010
2012
2014
2016
Time
GPPDNS
GPPNNS

784

785 Fig. 7

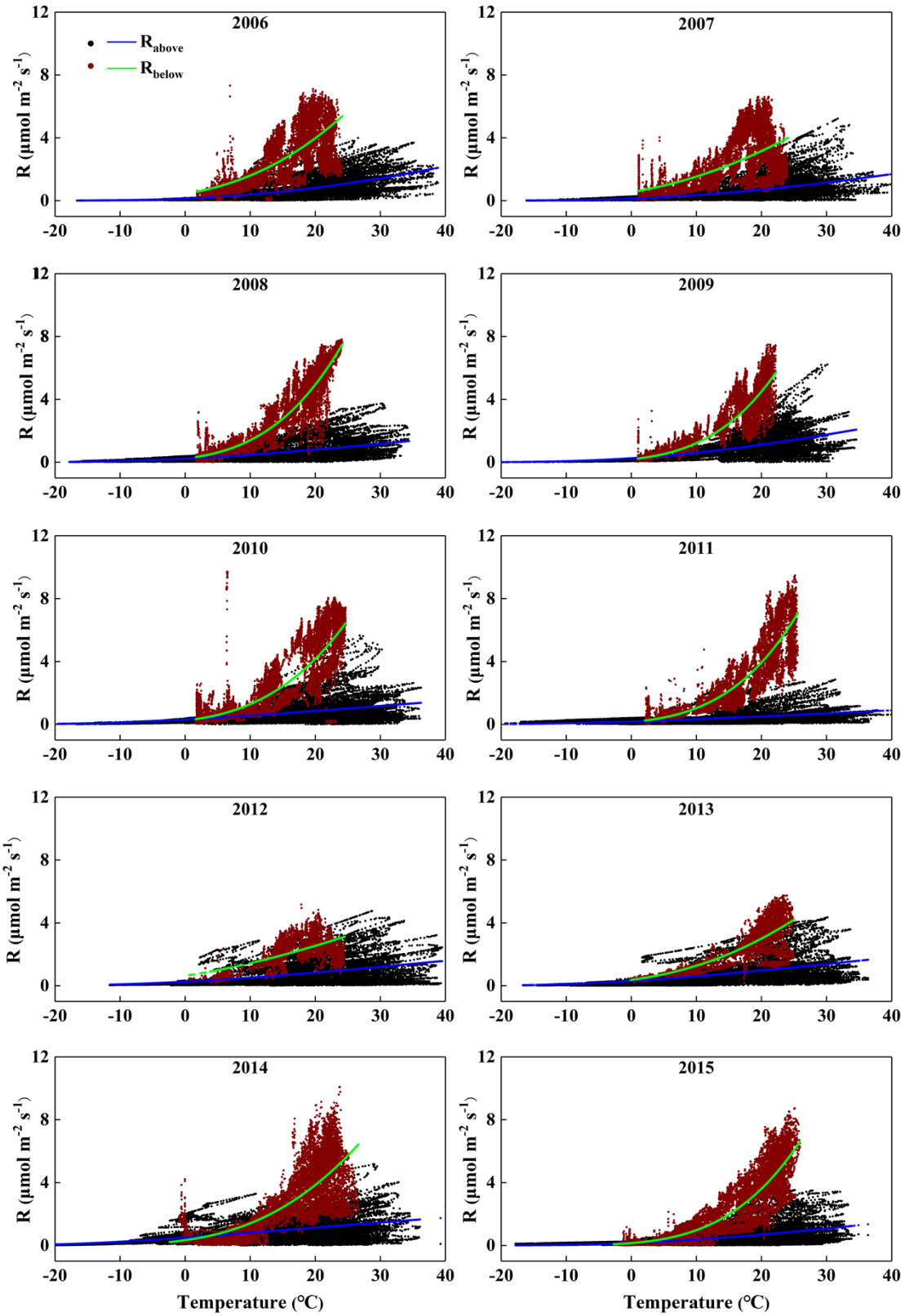

786
787

788 Fig. 8

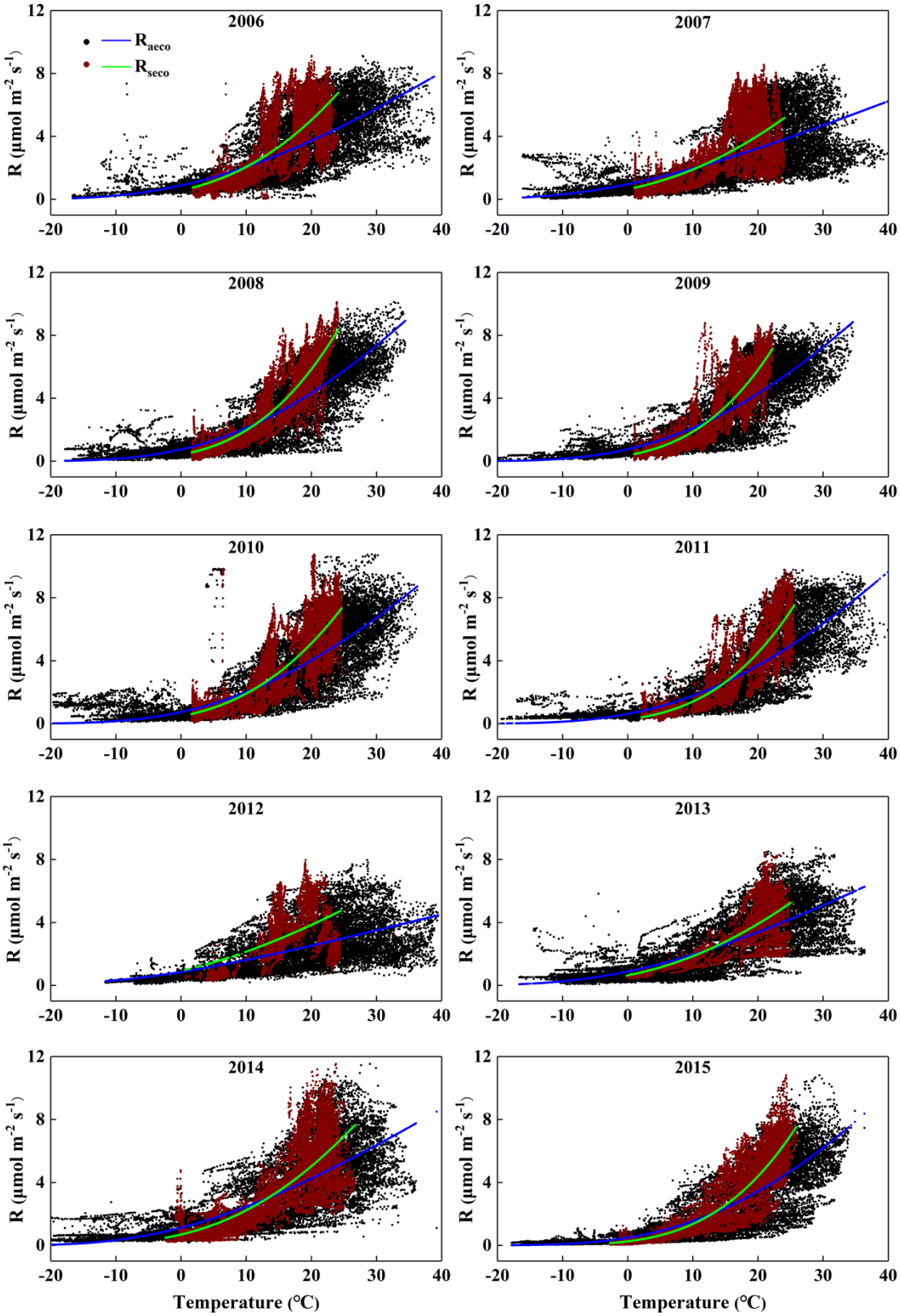

789
790

791 Fig. 9

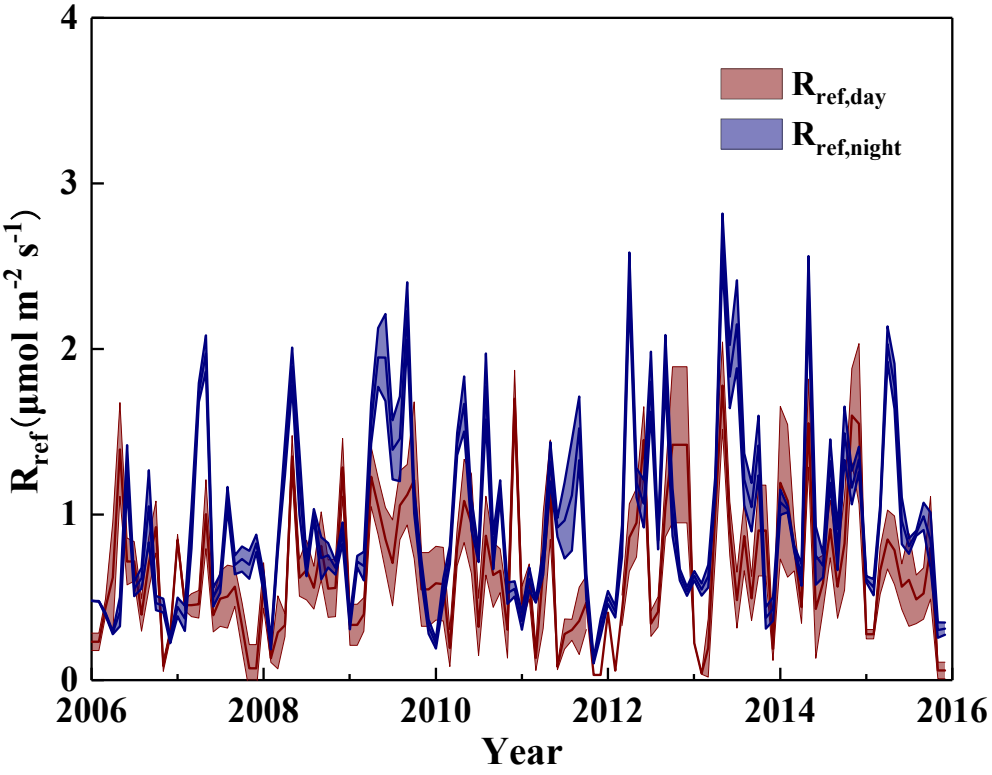
R_ref,day
R_ref,night
R_ref(μmol m^-2 s^-1)
Year
0
1
2
3
4
2006
2008
2010
2012
2014
2016

792

793 Fig. 10

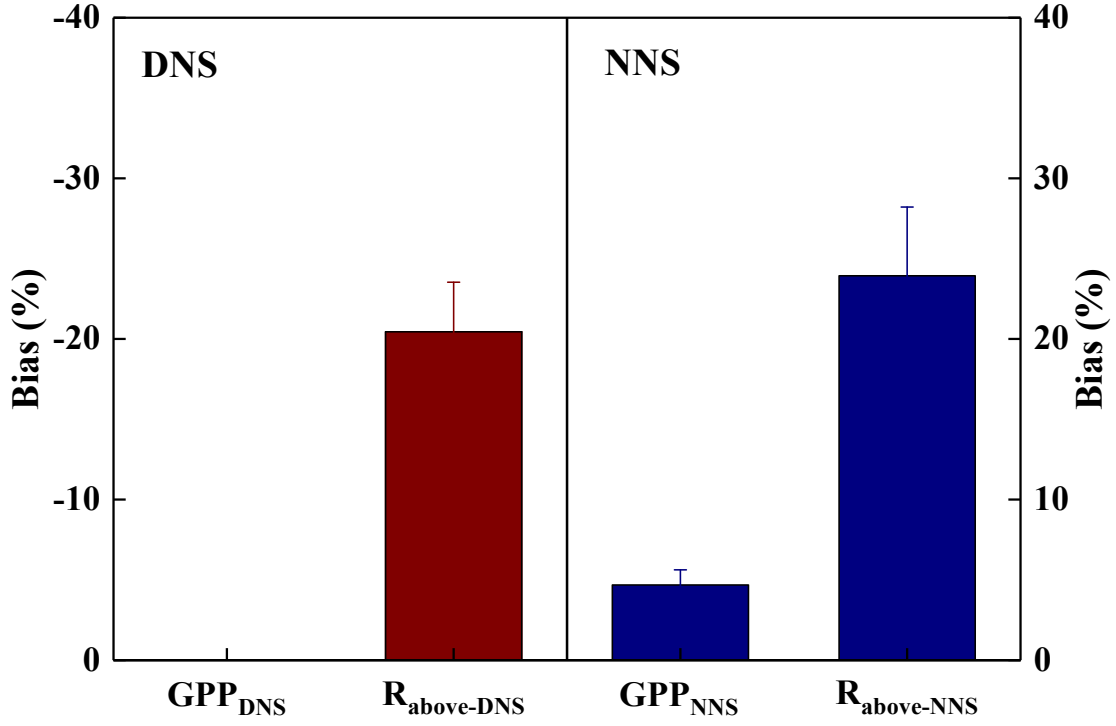

794

Table 1

Estimated above- (R_{above}) and belowground respiration (R_{below}), and GPP of growing season, non-growing season, and whole year from 2006 to 2015.

	Whole year			Growing season					Non-growing season		
	$R_{above\text{-}DNS}$	**$R_{above\text{-}NNS}$**	**R_{below}**	**$R_{above\text{-}DNS}$**	**$R_{above\text{-}NNS}$**	**R_{below}**	**GPP_{DNS}**	**GPP_{NNS}**	**$R_{above\text{-}DNS}$**	**$R_{above\text{-}NNS}$**	**R_{below}**
2006	0.65±0.04	0.63±0.03	2.38±0.09	1.00±0.05	0.97±0.05	3.65±0.11	6.36±0.24	6.46±0.25	0.30±0.03	0.29±0.01	1.09±0.06
2007	0.57±0.03	0.96±0.04	2.11±0.09	0.89±0.06	1.25±0.06	3.29±0.11	5.79±0.25	6.14±0.25	0.25±0.02	0.66±0.05	0.91±0.04
2008	0.61±0.03	0.91±0.04	2.52±0.11	0.92±0.05	1.28±0.05	4.27±0.11	7.35±0.23	7.79±0.24	0.28±0.02	0.53±0.03	0.76±0.04
2009	0.81±0.04	1.29±0.06	2.25±0.09	1.21±0.05	2.02±0.08	3.64±0.11	7.43±0.26	8.10±0.27	0.40±0.05	0.56±0.04	0.83±0.04
2010	0.69±0.04	1.04±0.05	2.55±0.11	1.04±0.06	1.55±0.06	4.11±0.14	7.12±0.23	7.66±0.23	0.35±0.02	0.52±0.04	0.97±0.06
2011	0.39±0.02	0.85±0.05	2.47±0.12	0.56±0.03	1.38±0.08	4.07±0.16	6.16±0.24	7.10±0.27	0.22±0.03	0.31±0.02	0.85±0.04
2012	0.73±0.04	1.29±0.05	1.47±0.05	1.11±0.07	1.76±0.07	1.96±0.07	4.25±0.23	4.68±0.22	0.34±0.03	0.81±0.06	0.99±0.06
2013	0.73±0.04	1.31±0.06	1.82±0.07	1.12±0.06	2.17±0.09	2.94±0.09	6.62±0.21	7.41±0.23	0.34±0.04	0.43±0.03	0.69±0.03
2014	0.92±0.04	1.08±0.05	2.31±0.11	1.24±0.06	1.56±0.08	3.98±0.12	6.51±0.23	6.87±0.22	0.59±0.04	0.59±0.02	0.61±0.04
2015	0.55±0.03	1.00±0.04	2.17±0.10	0.80±0.05	1.34±0.05	3.65±0.12	6.03±0.20	6.61±0.21	0.29±0.03	0.66±0.05	0.67±0.05
Average	0.67±0.04	1.04±0.05	2.21±0.09	0.99±0.06	1.53±0.07	3.55±0.11	6.36±0.23	6.88±0.24	0.34±0.03	0.54±0.04	0.84±0.05

$R_{above\text{-}DNS}$ (g C m^{-2} d^{-1}) and GPP_{DNS} (g C m^{-2} d^{-1}): estimated aboveground respiration and GPP using daytime NEE and soil respiration (DNS) method; $R_{above\text{-}NNS}$ (g C m^{-2} d^{-1}) and GPP_{NNS} (g C m^{-2} d^{-1}): estimated aboveground respiration and GPP using nighttime daytime NEE and soil respiration (NNS) method; R_{below} (g C m^{-2} d^{-1}): soil respiration.

Table 2

Response of aboveground respiration (R_{above}) to air temperature, and belowground respiration (R_{below}) to soil temperature.

		DNS method		NNS method			Measured value	
		E_0	R^2	E_0	R^2		E_0	R^2
2006	R_{above}	278±3.37	0.415	238±3.20	0.348	R_{below}	338±2.48	0.650
2007	R_{above}	251±4.31	0.303	162±2.24	0.371	R_{below}	268±3.21	0.443
2008	R_{above}	191±3.06	0.304	155±2.12	0.370	R_{below}	467±2.07	0.882
2009	R_{above}	227±3.26	0.358	219±2.64	0.451	R_{below}	484±2.49	0.835
2010	R_{above}	158±3.28	0.224	189±2.33	0.461	R_{below}	436±3.14	0.718
2011	R_{above}	162±3.99	0.157	189±3.68	0.267	R_{below}	496±3.13	0.818
2012	R_{above}	181±3.81	0.193	200±2.35	0.414	R_{below}	212±3.46	0.490
2013	R_{above}	176±3.25	0.257	207±2.56	0.447	R_{below}	317±4.72	0.638
2014	R_{above}	126±2.32	0.231	138±2.30	0.277	R_{below}	372±3.74	0.668
2015	R_{above}	224±4.47	0.230	161±2.37	0.346	R_{below}	486±3.44	0.799
Average	R_{above}	197±14.8A		186±9.95a		R_{below}	388±32.0Bb	

Different uppercase or lowercase letters indicate significant differences between temperature sensitivity of R_{above}, R_{below}. DNS method: daytime NEE and soil respiration method; NNS method: nighttime NEE and soil respiration method; R_{above} (μmol m^{-2} s^{-1}): aboveground respiration; R_{below} (μmol m^{-2} s^{-1}): belowground respiration; R_{ref} (μmol m^{-2} s^{-1}) : the basal respiration at reference temperature (T_{ref}) of 15°C; E_0 (K): temperature sensitivity.

Table 3

Response of ecosystem respiration (R_{eco}) to air and soil temperature.

	DNS method				NNS method			
	R_{aeco}		R_{seco}		R_{aeco}		R_{seco}	
	E_0	R^2	E_0	R^2	E_0	R^2	E_0	R^2
2006	220±1.78	0.599	332±2.40	0.656	212±1.80	0.570	341±2.30	0.685
2007	186±2.02	0.500	281±2.92	0.509	169±1.63	0.547	244±2.41	0.519
2008	267±1.68	0.758	404±1.87	0.858	246±1.50	0.768	371±1.75	0.845
2009	264±1.68	0.738	418±2.16	0.821	254±1.69	0.725	406±2.10	0.821
2010	259±1.99	0.686	364±2.45	0.725	261±1.79	0.734	363±2.23	0.761
2011	273±1.99	0.719	433±2.72	0.806	260±2.11	0.678	423±2.92	0.775
2012	165±1.90	0.426	217±4.15	0.419	175±1.53	0.561	203±2.99	0.541
2013	205±1.74	0.616	276±4.49	0.576	214±1.77	0.633	312±4.97	0.606
2014	203±1.89	0.582	302±2.82	0.656	202±1.76	0.619	297±2.57	0.690
2015	297±2.40	0.652	434±2.70	0.807	261±1.93	0.687	378±2.09	0.830
Average	234±13.8A		346±24.1B		225±11.3a		334±22.2b	

Different uppercase or lowercase letters indicate significant differences between air and soil temperature sensitivity of R_{eco}. DNS method: daytime NEE and soil respiration method; NNS method: nighttime NEE and soil respiration method; R_{aeco}: air temperature sensitivity of ecosystem respiration; R_{seco}: soil temperature sensitivity of ecosystem respiration; R_{ref} (μmol m^{-2} s^{-1}) : the basal respiration at reference temperature (T_{ref}) of 15°C; E_0 (K): temperature sensitivity.